Favorable Pendant-Amino Metal Chelation in VX Nerve Agent Model Systems

Indrajit Bandyopadhyay, Min Jeong Kim, Yoon Sup Lee,* and David G. Churchill*

Department of Chemistry and School of Molecular Science (BK 21), Korea Advanced Institute of Science and Technology, Daejeon, 305-701 Republic of Korea

Received: September 9, 2005; In Final Form: November 17, 2005

We have performed DFT computational studies [B3LYP, 6-31+G*] to obtain metal ion coordination isomers of VX-Me [MeP(O)(OMe)($SCH_2CH_2NMe_2$)], a model of two of the most lethal nerve agents: VX [MeP(O)(OEt)($SCH_2CH_2N(^iPr)_2$)] and Russian-VX [MeP(O)(OCH_2CHMe_2)($SCH_2CH_2N(Et)_2$)]. Our calculations involved geometry optimizations of the neutral VX-Me model as well as complexes with H^+, Li^+, Na^+, K^+, Be^{2+}, Mg^{2+}, and Ca^{2+} that yielded 2−8 different stable chelation modes for each ion that involved mainly mono- and bidentate binding. Importantly, our studies revealed that the [O_P,N] bidentate binding mode, long thought to be the active mode in differentiating the hydrolytic path of VX from other nerve agents, was the most stable for all ions studied here. Binding energy depended mainly on ionic size as well as charge, with binding energies ranging from 364 kcal mol^{-1} for Be^{2+} to 33 kcal mol^{-1} for K^+. Furthermore, calculated NMR shifts for VX-Me correlate to experimental values of VX.

1. Introduction

Organophosphate nerve agents are stockpiled worldwide.[1] Presently, they are disposed of by either incineration or hydrolysis. Deployment of such agents during peacetime in Japan[2−4] and wartime in Iraq[5−7] supports the need for continued research into real-time sensor technology and decontamination systems[8−10] for nerve agents such as sarin and VX [(*O*-ethyl-*S*-[diisopropylamino]ethyl)methylphosphonothioate]. The effect of metal coordination on P−X (X = O, S) and C−S bond cleavage is thus as relevant as ever. P−S bond cleavage is essential in decontamination and thus is most sought; C−S cleavage proves to be difficult to achieve; and P−OR bond hydrolysis produces the undesired and still highly toxic thiocolic acid derivative.[8,9] There are various VX isomers, namely, two constitutional isomers, VX [MeP(O)(OEt)($SCH_2CH_2N(^iPr)_2$)] and Russian-VX [MeP(O)(OCH_2CHMe_2)($SCH_2CH_2N(Et)_2$)] (Figure 1), each of which possess a stereogenic center. However, toxicity is extreme regardless of the isomer.[8,11]

Various modeling approaches continue to be undertaken. Previous computational studies have been performed on VX[12,13] and related organophosphates[14−18] but these efforts have not addressed agent binding and the determination of stable coordination isomers that enable VX to be positioned for selective bond cleavage.

It is hypothesized that VX−metal binding is distinct from G-type organophosphates by virtue of an additional interaction with the tertiary nitrogen. Can, therefore, VX function as a bidentate ligand (Figure 1)?[8] To address this question, we have engaged in model studies to establish the fundamental coordination chemistry of VX with a single metal ion center. Thus, there are hard and soft donor atoms of varying hybridization combined with extremely low symmetry. VX−sulfur binding has been previously addressed.[19] Implications of modeling such metalation are varied and include design of ligand systems that allow for selective VX binding and selective hydrolysis,[13] sensing, as well as insight into metalloenzyme-mediated detoxification.

Reports of VX in the presence of the ions/compounds of sodium,[20] magnesium,[21] aluminum,[20] manganese,[22] copper,[23] silver,[19] zinc,[24] and europium[25] have been made. Despite numerous related reports, there are still no known structural examples of M−VX interactions to the best of our knowledge, frustrating in light of the proposition that metal binding mediates nucleophilic displacement at phosphorus.[8,26] VX chemistry is diverse. Furthermore VX itself can be composed of the P_S and P_R enantiomers. Here, we have used (P_S) VX-Me which possesses a greater acetylcholine toxicity in biology than the P_R isomer.[11] VX has been modified in this report to possess methyl groups in place of ethoxy and diisopropyl units (Figure 1). Gas phase calculations are relevant especially to technologies in which airborne analytes adsorb to metal ions.[27,28] Gas phase calculations also provide information about agent activity in some solution matrixes. Neat VX is an organic material, soluble in aqueous alkali solution only at low concentrations,[8] and cations present in alkaline media may participate in bonding as a result of metal coordination.

The synthetic preparation of known simulants has allowed for experimental handling that is less stringent, however, only partial information of the wide range of the complex methyl phosphonothioate chemistry of VX is true for these mimics (Figure 3).[8] By inspection of the structures in Figure 3, none of these mimics provide for "the unique intramolecular amino nitrogen effect" found in VX.[8] Demeton-S-ethyl has the most likeness to VX, however the [S-Et] unit is likely to exhibit significantly different chemistry than the [-N($CH(CH_3)_2)_2$] unit. Additionally, the [P-O-Et] unit has formally replaced the [P-Me] group.

2. Computational Details

Geometries were optimized with density functional theory (DFT) methods using combined Becke's three parameter exchange functional and the gradient-corrected correlation functional of Lee, Yang, and Parr, known as the B3LYP method,[29,30] in conjunction with the standard 6-31+G* basis set. All input geometries were optimized without constraints.

* To whom correspondence should be addressed. (Y.S.L.) E-mail: yslee@mail.kaist.ac.kr. Phone: 82-42-869-2821. (D.G.C.) E-mail: dchurchill@kaist.ac.kr. Phone: 82-42-869-2845. Fax: 82-42-869-2810.

10.1021/jp055112x CCC: $33.50 © 2006 American Chemical Society
Published on Web 02/21/2006

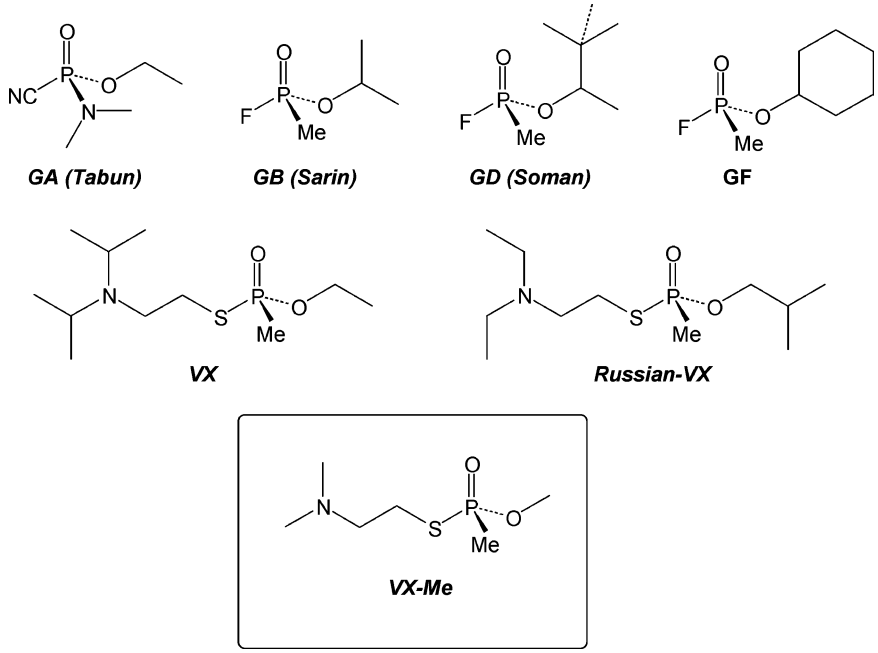

Figure 1. G- and V-type nerve agents (undesignated stereocenters).

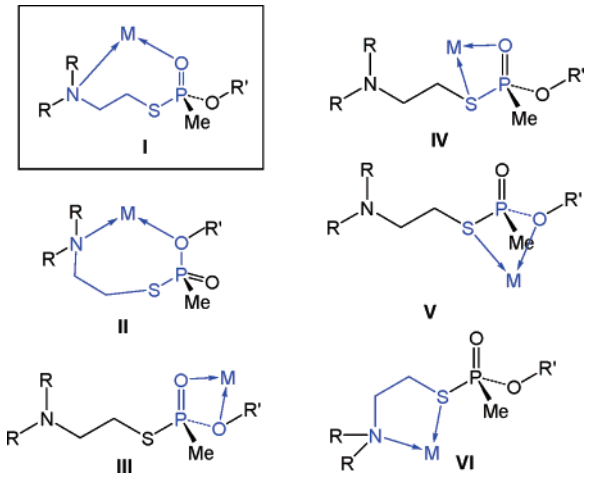

Figure 2. Six proposed bidentate binding modes for VX, R = ^{i}Pr, R′ = Et and Russian-VX, R = Et, R′ = CH_2-^{i}Pr.

Vibrational frequencies were calculated for structures **1**−**35**. Imaginary frequencies were absent in all structures reported here indicating true minima were located. Structural parameter and certain mode-specific frequencies are compared with available experimental values where possible. The basis set superposition errors (BSSE) were calculated using standard counterpoise correction of Boys and Bernardi.[31] Binding energies were calculated as the difference in energy for a given complex geometry, and the calculated energies for geometry **1** and the corresponding M^{n+} and are given as positive values. The binding energies have been modified to account for thermal correction at $T = 298$ K and $P = 1$ atm. Corrected and uncorrected energies are provided in Tables 1 and 3. All calculations were performed with the Gaussian 03 suite of programs.[32]

To examine the effect of dispersion interactions and to establish consistency between the computational methodologies, we also undertook MP2 calculations for the most stable complexes. These values are in parentheses in Tables 1 and 2 and the Cartesian coordinates are provided in the Supporting Information. Single-point energy calculations [CCSD(T)/6-31+G*//MP2/6-31+G*] were also performed on select geometries. Basis set effects were also investigated for several complexes at the DFT level employing 6-311++G** basis sets.

3. Results and Discussion

The geometry of the neutral VX−Me model system was optimized and appears in Figure 4. Its two flexible arms [-OMe] and [-SR] rotate in a way similar to a related structurally characterized substrate.[33] In the geometry of VX−Me, the O−P−O−Me dihedral angle is 47°, the O═P−S−C angle is ca. 11°, the N−C−C−S angle is 177°, and the C−C−S−P angle is ca. 88°.

Notably in **1**, the O_P,N binding atoms are not arranged for metal chelation (O_P···N distance = 4.43 Å);[34] stability is gained when the dimethylene unit between the S and N atoms achieves the anti configuration. Since this geometry is taken to be the most stable conformation, some organization is required prior to complexation, evident from the geometry optimized VX complexes provided in Figures 5 and 6.

The simplest and most common chelation occurs by way of protonation (Figure 5), most greatly favored at nitrogen. Additional stability is imparted by the proximal phosphoryl oxygen, allowing for the formation of an intramolecular hydrogen bond in geometry 2.

This bidentate coordination is also favored for alkali and alkaline earth metal ions. Loss of the amino contact as in geometry **3** destabilizes this geometry by 26.3 kcal mol^{-1} as indicated by the differences in the binding energy values appearing in Table 1. More about the properties of the complexes involving the proton is discussed subsequently.

The optimized metal complex geometries are arranged from greatest to least stability by ion (Figures 6 and 7); geometric/energetic values are summarized in Tables 1 and 2. The exhaustive list of M···X (X = N, O, S) internuclear distances below reveals a correlation between O_P,N bidenticity and stability. Notably, the stable conformers for Li^+ (**5**), Na^+ (**11**), and K^+ (**19**) all involve a bidentate O_P,N metal interaction, e.g., in geometry **5** the [Li···O═P] distance is 1.78 Å and the [Li···N] distance is 2.02 Å. We see comparable geometric parameters for Na^+ and K^+ complexes: the [Na···O═P] distance in geometry **11** is 2.18 Å and the [Na···N] distance is 2.39 Å.

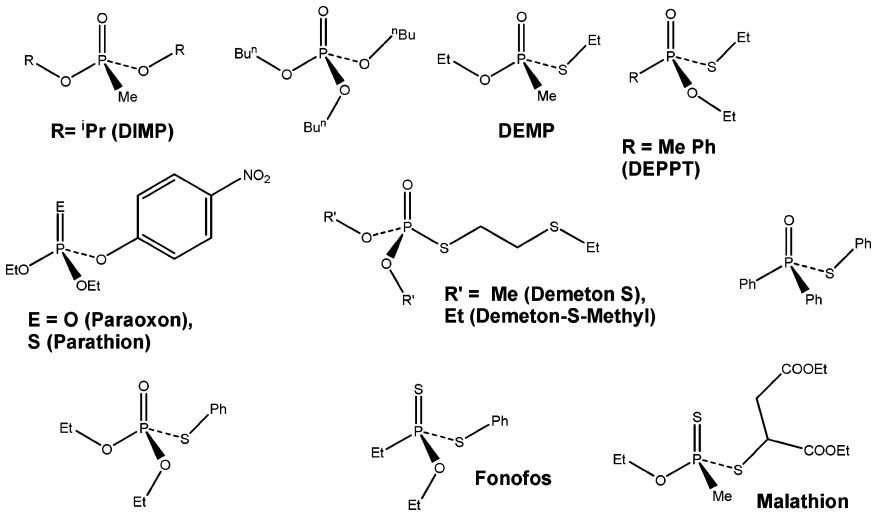

Figure 3. Illustrations of VX simulants adapted from ref 9.

TABLE 1: Internuclear Distances and Binding Energies (BE, kcal mol^{-1}) of M$^+$−VX−Me Complexes Optimized at the B3LYP/6-31+G* Level[a]

ion	geom.	M$^+$···O=P	M$^+$···N	M$^+$···O	M$^+$···S	BE	BE+ BSSE	BE+Th. Corr.*
H$^+$	**2**	**1.71**	**1.05**	3.73	2.98	**246.4**	**245.8**	**237.7**
		(1.76)	**(1.05)**	(3.65)	(2.87)	**(247.3)**	**(245.2)**	**(237.3)**
H$^+$	**3**	**0.98**	5.55	2.77	3.30	**220.1**	**220.0**	**214.0**
H$^+$	**4**	3.46	5.38	**0.98**	3.04	**197.4**	**197.1**	**191.0**
Li$^+$	**5**	**1.78**	**2.02**	3.81	3.29	**76.3**	**75.1**	**73.6**
		(1.84)	**(2.03)**	(3.65)	(3.00)	**(75.9)**	**(71.1)**	**(70.0)**
Li$^+$	**6**	3.63	**2.02**	**1.94**	**2.52**	**68.9**	**67.5**	**66.2**
Li$^+$	**7**	**1.72**	8.33	4.21	4.22	**59.1**	**58.3**	**57.5**
Li$^+$	**8**	**1.73**	3.42	4.27	4.20	**58.8**	**58.0**	**57.3**
Li$^+$	**9**	**1.84**	5.04	**2.06**	4.20	**56.2**	**55.2**	**54.5**
Li$^+$	**10**	3.80	4.45	**1.89**	**2.46**	**45.3**	**44.2**	**43.8**
Na$^+$	**11**	**2.18**	**2.39**	4.19	3.23	**53.8**	**52.2**	**51.3**
		(2.24)	**(2.43)**	(4.18)	(3.23)	**(52.2)**	**(48.2)**	**(47.5)**
Na$^+$	**12**	3.90	**2.40**	**2.34**	**2.81**	**47.6**	**45.8**	**44.9**
Na$^+$	**13**	**2.09**	8.64	4.60	4.52	**43.5**	**42.2**	**41.6**
Na$^+$	**14**	**2.09**	7.01	4.04	4.79	**41.8**	**40.7**	**40.4**
Na$^+$	**15**	**2.10**	4.02	4.60	4.74	**41.6**	**40.2**	**39.9**
Na$^+$	**16**	**2.19**	5.10	**2.47**	4.58	**40.5**	**39.1**	**38.8**
Na$^+$	**17**	5.66	**2.39**	5.12	**2.70**	**39.0**	**37.9**	**37.5**
Na$^+$	**18**	4.13	4.58	**2.29**	**2.79**	**30.9**	**29.6**	**29.3**
K$^+$	**19**	**2.58**	**2.91**	4.06	3.67	**34.9**	**33.9**	**33.3**
		(2.64)	**(2.87)**	(3.27)	(3.62)	**(39.4)**	**(33.3)**	**(32.8)**
K$^+$	**20**	**2.47**	8.94	4.95	4.83	**31.7**	**31.1**	**30.6**
K$^+$	**21**	4.20	**2.87**	**2.82**	**3.24**	**30.1**	**29.1**	**28.8**
K$^+$	**22**	**2.48**	4.92	4.87	5.29	**28.2**	**27.3**	**27.0**
K$^+$	**23**	**2.56**	5.38	3.03	5.09	**29.3**	**28.6**	**28.2**
K$^+$	**24**	**2.50**	4.65	4.76	4.87	**27.1**	**26.5**	**26.1**
K$^+$	**25**	6.07	**2.89**	5.31	**3.12**	**25.0**	**24.2**	**24.1**

[a] Values in paretheses are optimized at the MP2/6-31+G*. BSSE = basis set superposition error is calculated by the counterpoise method. The asterisk (*) indicates (incl. ZPE) + BSSE. Th. Corr. = Thermal correction from 0 to 298 K, ZPE = zero-point energy. Distances in bold indicate bond formation. Interactions are judged by comparing calculated distances to reference distances.[35,45] M = H, Li, Na, and K. Thermal correction in the last column refers to the thermal correction to energy (E_{tot}) which equals the sum of E_{tr}, E_{rot}, and E_{vib} (tr: translational, rot: rotational, vib: vibrational). For metal ions, thermal correction (E_{tr}+ E_{rot},) equals 2.5*RT*.

Likewise for **19**, the [K···O=P] distance is 2.58 Å and the [K···N] distance is 2.91 Å. Metal bonding to N and O gives rise to stability rationalized by a Lewis acidic metal ion optimizing binding from the Lewis basic heteroatoms through unstrained conformational change of the VX−Me ligand. Thus monodentate interactions are less favored, and binding modes V and VI (Figure 2) featuring strained four-membered chelate rings are also less favored.

The VX−Me−alkaline earth metal ion (Be^{2+}, Mg^{2+}, Ca^{2+}) complexes below in Figure 7 reveal similar patterns to what is observed for those of the alkali metals above. Notably, geometries **26**, **28**, and **31** represent the most stable binding energy conformers.

The geometries reflecting lowest energy structures in Tables 1 and 2 were then geometry optimized again using the MP2/6-31+G* basis set giving very similar, if not exact energetic and geometric values (shown in parentheses). This was done in order to benchmark these calculations to assist in future theoretical comparisons. Furthermore, single-point energy calculations [CCSD(T)/6-31+G*//MP2/6-31+G*] were also performed on geometries **2** for H^+ (248.8 kcal/mol), **5** for Li^+ (76.6 kcal/mol), **11** for Na^+ (52.7 kcal/mol), **19** for K^+ (40.0 kcal/mol), **26** for Be^+ (367.5 kcal/mol), **28** for Mg^+ (219.0 kcal/mol), and **31** for Ca^{2+} (143.3 kcal/mol) giving binding energies in good agreement with those obtained at the B3LYP/6-31+G* level. To investigate the basis set effect on the binding energies,

TABLE 2: Metal Ion−Heteroatom Internuclear Distances and Binding Energies (BE, kcal mol^{-1}) of M^{2+}−VX−Me Complexes Optimized at the B3LYP/6-31+G* Level[a]

metal ion	geometry	M^{2+}···O═P (Å)	M^{2+}···N (Å)	M^{2+}···O (Å)	M^{2+}···S (Å)	BE	BE+ BSSE	BE+Th. Corr.(incl.ZPE)
Be^{2+}	**26**	**1.52**	**1.66**	3.34	**2.18**	**368.7**	**366.7**	**364.4**
		(1.54)	**(1.67)**	(3.31)	**(2.13)**	**(365.3)**	**(355.0)**	**(353.2)**
Be^{2+}	**27**	3.32	**1.67**	**1.57**	**2.07**	**350.2**	**348.0**	**347.8**
Mg^{2+}	**28**	**1.93**	**2.10**	3.66	**2.59**	**223.9**	**221.8**	**220.6**
		(1.95)	**(2.10)**	(3.62)	**(2.60)**	**(217.9)**	**(210.1)**	**(209.2)**
Mg^{2+}	**29**	3.57	**2.09**	**2.01**	**2.46**	**207.5**	**205.2**	**204.1**
Mg^{2+}	**30**	**1.94**	6.66	**2.14**	4.14	**174.4**	**172.9**	**172.9**
Ca^{2+}	**31**	**2.26**	**2.51**	3.99	3.09	**142.6**	**141.3**	**140.4**
		(2.28)	**(2.50)**	(3.91)	(3.12)	**(142.5)**	**(135.9)**	**(135.2)**
Ca^{2+}	**32**	3.89	**2.49**	**2.39**	**2.88**	**126.9**	**125.6**	**125.3**
Ca^{2+}	**33**	**2.17**	3.97	4.65	4.59	**116.1**	**115.1**	**115.9**
Ca^{2+}	**34**	**2.26**	3.92	**2.46**	4.45	**114.4**	**113.2**	**113.7**
Ca^{2+}	**35**	**2.22**	6.84	4.46	2.95	**109.4**	**108.6**	**108.9**

[a] Values in parentheses are optimized at the MP2/6-31+G*. The content of the footnote for Table 1 applies here as well. M = Be, Mg, and Ca.

TABLE 3: Geometric Parameters of the [O···M^{n+}···N] (n = 1, 2) Interaction[a]

geometry	description	[O···N] distance (Å)	[O···M^{n}+···N] angle (°)
2	[H^+−VX−Me]	2.70	154.6
5	[Li^+−VX−Me]	3.41	127.8
11	[Na^+−VX−Me]	3.93	118.3
19	[K^+−VX−Me]	3.92	90.9
26	[Be^{2+}−VX−Me]	2.97	137.5
28	[Mg^{2+}−VX−Me]	3.63	129.1
31	[Ca^{2+}−VX−Me]	3.92	110.6

[a] M = H^+, Li^+, Na^+, K^+, Be^{2+}, Mg^{2+}, and Ca^{2+}.

single-point calculations [B3LYP/6-311++G**//B3LYP/6-31+G*] were carried out on structures **2** for H^+ (247.0 kcal/mol), **5** for Li^+ (76.8 kcal/mol), **11** for Na^+ (53.5 kcal/mol), **19** for K^+ (36.2 kcal/mol), **26** for Be^+ (368.9 kcal/mol), **28** for Mg^+ (223.9 kcal/mol), and **31** for Ca^{2+} (157.0 kcal/mol) giving binding energies in good agreement with those obtained at the B3LYP/6-31+G* level except in the case of Ca^{2+}.

We can now consider each stable complex that bears the [O_P,N] heteroatom−metal ion contact. The chelation bite angle

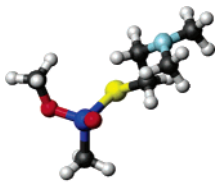

1

Figure 4. Geometry optimized structure of uncomplexed VX−Me (1). O = red, S = yellow, P = dark blue, C = dark gray, H = white, N = light blue.

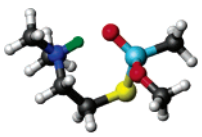

2

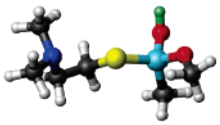

3

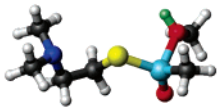

4

Figure 5. Geometry optimized structures of H^+−VX−Me. H^+ = green, O = red, S = yellow, N = dark blue, C = dark gray, H = white, P = light blue.

[O···M^{n+}···N] and the O···N distance of the ligand are easily modified to accommodate metals of various sizes. In particular, the [O···H^+···N] angle is ca. 155° with an [O···N] separation of 2.70 Å. Internuclear [O···N] distances and [O···M^{n+}···N] angles for the chelated metal ions range from 3.41 to 3.92 Å and ca. 91−138°, respectively (Table 3).

There are some structural fragments that are helpful in considering certain metal−VX binding modes. Complexes containing a neutral [$R_2N-CH_2-CH_2-S-R'$] fragment are known and these motifs are reminiscent of those in geometries **11** and **25** above.[36−40] In these structures, the R group does not contain subsequent chelating amino groups. There are also examples of [$R_2N-CH_2CH_2-S-$] LX-type metal complex derivatives which can be thought of as formally representing a coordinated thiocholine arm immobilized after hydrolysis.[41]

P═O, C−S, P−OR, and P−S bonds are often the intended target of hydrolysis in efforts to detoxify VX. Metalation effects these bonds. Compared to the most stable binding mode **I** (Figure 2) for all monocationic and dicationic complexes, P═O and C−S bonds undergo elongation, whereas P−OR and P−S bonds undergo contraction (except for divalent metals discussed below). The P═O bond has the maximum elongation for group II metal cations (Be^{2+}, 0.07; Mg^{2+}, 0.04; Ca^{2+}, 0.03 Å) compared with group I cations (H^+, 0.02; Li^+, 0.02; Na^+, 0.01; K^+, 0.003 Å), due to a greater electrostatic interaction. As for the P═O bond, the C−S bond decreases from Be^{2+} to Ca^{2+} in the second group (0.04, 0.04, and 0.02 Å). For Li^+ to K^+, the values are 0.01, 0.01, 0.01 Å.[42a] The contraction behavior of P−OR (Li^+, −0.03; Na^+, −0.03; K^+, −0.02; Be^{2+}, −0.08; Mg^{2+}, −0.06; Ca^{2+}, −0.05) is similar to P═O and C−S bonds. However, for the P−S bond, it undergoes contraction in the presence of group I metal ions (Li^+, −0.02; Na^+, 0.00; K^+, −0.01 Å) but elongation for dipositive metal ions (Be^{2+}, 0.05; Mg^{2+}, 0.05; Ca^{2+}, 0.02 Å) ascribed to a substantial M−S interaction.

For the next stable binding mode **II** (Figure 2), the extent of elongation of C−S bond (Å) decreases down the group (Li^+, 0.01; Na^+, 0.01; K^+, 0.01; and Be^{2+}, 0.04; Mg^{2+}, 0.03; Ca^{2+}, 0.02). Similarly, the contraction of the P═O bond (Å) either remains the same or decreases (Li^+, −0.01; Na^+, −0.01; K^+, −0.01; and Be^{2+}, −0.03; Mg^{2+}, −0.02; Ca^{2+}, −0.02). The P−OR bond length (Å) (Li^+, 0.05; Na^+, 0.04; K^+, 0.03 and Be^{2+}, 0.15; Mg^{2+}, 0.11; Ca^{2+}, 0.08) also decreases. The P−S bond undergoes elongation except for the K^+ ion (−0.04 Å) and the magnitude decreases down a group (Li^+, 0.01; Na^+, 0.004; Be^{2+}, 0.07; Mg^{2+}, 0.06; Ca^{2+}, 0.04 Å). For K^+, the P−S bond contracts due to the large size of K^+; the K^+···S interaction is thought to be weak with a distance of 3.24 Å. Despite bond

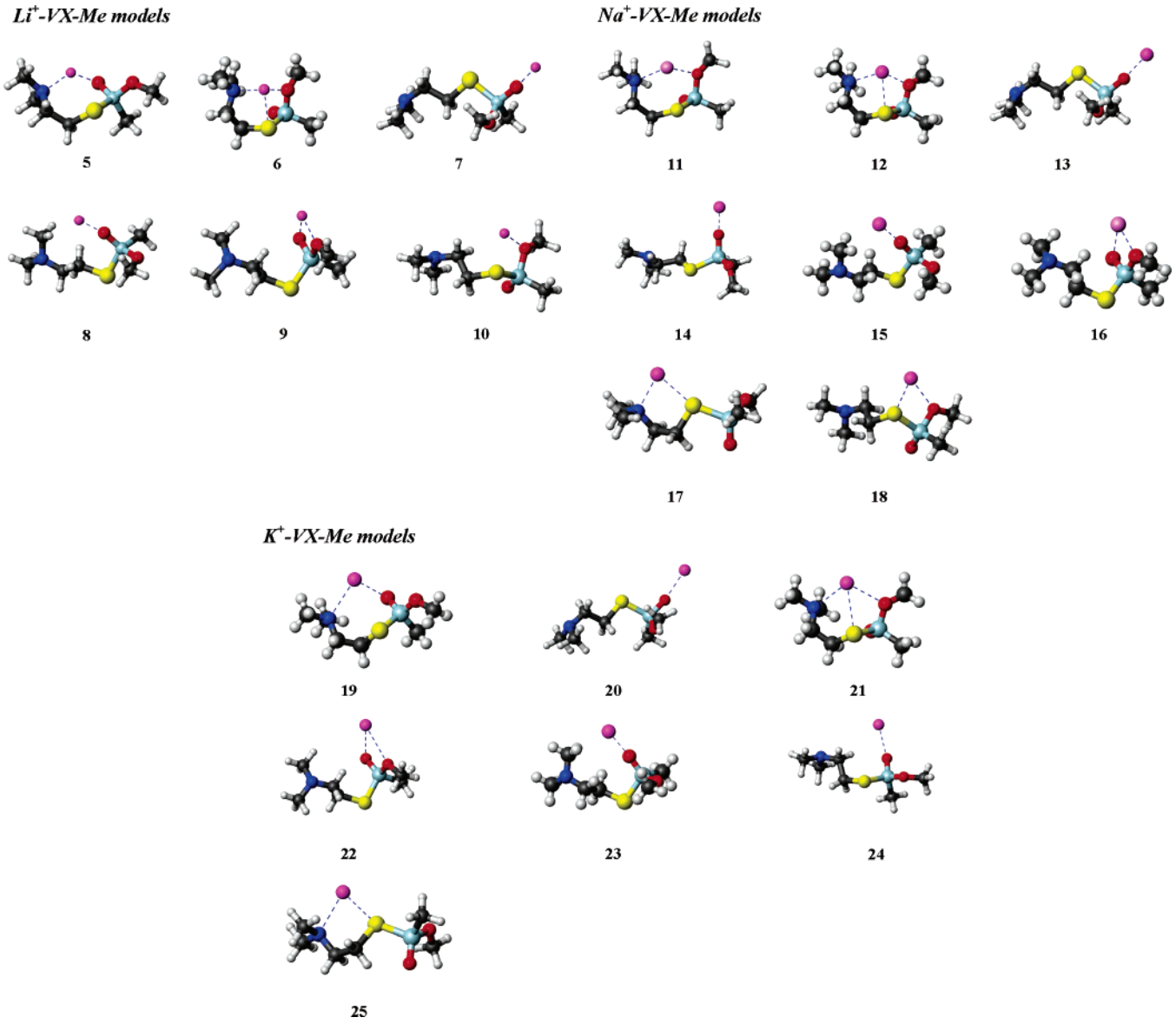

Figure 6. Geometry optimized $M^+-VX-Me$ complexes with Li^+, Na^+, and K^+. M^+ = dark pink, O = red, S = yellow, N = dark blue, C = dark gray, H = white, P = light blue. Interactions of M^+ with heteroatoms are represented by dotted lines.

elongations, the bidenticity may inhibit hydrolysis due to the conformational rigidity that the seven-membered chelate ring creates.

These model systems involve the simplest metal complex possible: a lone metal ion devoid of an ancillary ligand system. The result of these efforts is structural information with no real experimental counterparts for comparison. However, this information may be helpful in sensing technology. Sorption detection devices detect "gas phase" analytes and may use a polymer that is layered onto a surface of a quartz crystal. This coating may contain metal ions by design as sorption sites allowing for analyte/agent binding specificity through the formation of stable binding modalities. A bidentate VX arrangement seems realistic in practice, save for the conformational cost and requirement of adjacent vacant sites at a single metal ion. These criteria rule out the utility of single open-site complexes, as well as the presence of bulky ancillary ligands, judging from the bite angles appearing in Table 3. These angles do suggest, however, that heavier metals afford a narrower bite angle and will tolerate some bulky ancillary ligand support. Unfortunately from our modeling attempts thus far, we cannot speculate about which metal complex/ligand systems are suitable.

Spectroscopy. Theoretical calculations have enabled us to calculate the NMR shifts for all atoms in VX−Me.[42b] Although many of the proton signals for the model do not have direct counterparts in the actual VX and Russian-VX systems, we have compared certain relavent shifts that exist for both (Table 4). We also include a complete list of computed NMR shifts for $H^+-VX-Me$ and the metal complexes.

According to these calculations, upon metal complexation, the [P−Me] carbon signal moves to lower field, whereas the methylene carbons in the S−C−C−N pendant arm appear at slightly higher field. This trend in shifts upon metal complexation has been reported before experimentally for different systems.[45] These theoretical differences in chemical shift should allow for ease in spectroscopic detection experimentally. A complete table of NMR values is provided in the Supporting Information.

Additional spectroscopic information is provided by the O═P stretching band for the VX−Me ligand and complex. Much is known about the [M···O═PR_3] interaction; the phosphoryl stretch (ca. 1200 cm^{-1}) serves as a useful reporter of the strength of the metal−oxygen interaction.[46,47] However few structural studies have been performed on groups other than O═PR_3 moieties (R = alkyl, aryl). From a survey of those structures in

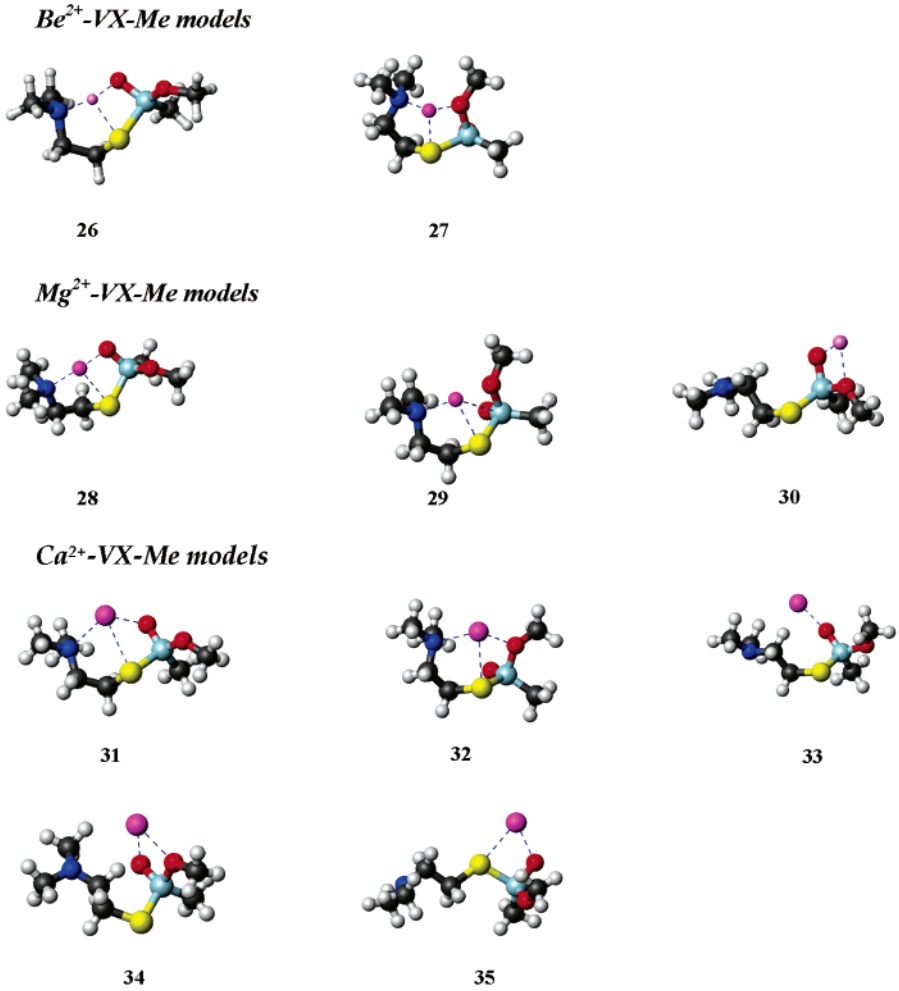

Figure 7. Geometry optimized VX−Me complexes Be^{2+}, Mg^{2+}, and Ca^{2+}. M^{2+} is dark pink, O = red, S = yellow, N = dark blue, C = dark gray, H = white, P = light blue. Interactions of M^{2+} with heteroatoms are represented by dotted lines.

TABLE 4: ^{31}P and ^{13}C NMR Isotropic Chemical Shifts (Relative to TMS; All Values in ppm) for the Most Stable Protonated (2) and Other Metalated Complexes at GIAO−B3LYP/6-31+G*

	1	VX	**2** (H^+)	**5** (Li^+)	**11** (Na^+)	**19** (K^+)	**26** (Be^{2+})	**28** (Mg^{2+})	**31** (Ca^{2+})
***P*(CH$_3$)**[a]	54.0	52.4[a] 61.7[1,b] 55.4[2,b] 57.0[3,b]	147.7	67.7	65.5	58.4	86.3	83.6	74.6
P(*C*H$_3$)	18.2	23.6[a] 17.6[b,1]	20.56	11.9	14.5	12.5	11.5	11.0	11.0
SCH$_2$	25.3	34.1[a] 25.3[b,1]	54.0	27.4	27.9	27.4	36.7	32.3	29.3
NCH$_2$	57.7	47.7[a] 47.3[b,1]	40.7	58.7	56.2	56.2	57.8	55.6	56.3

[a] Reference 43. The external reference for the ^{31}P value was 85% phosphoric acid. [b] Reference 44. 1, water; 2, *tert*-butyl alcohol; 3, $CDCl_3$.

the Cambridge Structural Database, the mean P−O bond length in [M···O═P] interactions is 1.50 Å, and the mean [M···O] distance is 2.09 Å.[48] Electron-poor ions (e.g., Fe^{3+} and Cu^{2+}) favor strong coordination with a concomitant change in [O═P] stretching frequency by 30−100 cm^{-1}. The computed [P═O] stretching frequency for **1** is 1181.0 cm^{-1}. Additionally, the derivatives for Li^+ (**5**) and Na^+ (**11**) give lower energy stretches of 1125.8 and 1163 cm^{-1}, respectively, rationalized by the weakening of the [O═P] bond in creating the [M···O═P] electrostatic interaction. For Be^{2+} and Mg^{2+}, P═O stretches are dramatically red-shifted to 927 and 938 cm^{-1}, respectively, indicating a strong [M···O═P] electrostatic interaction in their respective complexes (**26** and **28**) due to their divalent nature and small size.

4. Conclusion

We have modeled metal ion coordination isomerism involving VX−Me [MeP(O)(OMe)($SCH_2CH_2NMe_2$)], a model that bears very close resemblance to both VX [MeP(O)(OEt)($SCH_2CH_2N(^iPr)_2$)] and Russian-VX [MeP(O)(OCH_2CHMe_2)($SCH_2CH_2N(Et)_2$)] which are stockpiled in the United States and in Russia, respectively. Our DFT computational [B3LYP, 6-31+G*] studies point to secondary amino coordination at a single metal center that serves to stabilize the primary monodentate M−O binding mode of VX−Me. Thus, VX can be considered a bidentate ligand, important in further sensing and decontamination studies. Geometry optimizations of the neutral VX−Me as well as complexes with H^+, Li^+, Na^+, K^+, Be^{2+}, Mg^{2+}, and Ca^{2+} were obtained. Theoretical binding studies show a preference for VX [O_P,N] chelation involving a seven-membered chelate ring for all ions examined here. Thus, when considering ligand design, this coordination suggests the need for a minimum of two adjacent open sites at one metal ion in a given metal ion or complex that accommodates [O_P···M···N] bite angles that

are seen to decrease for the heavier ions for both groups I and II. Binding energies mainly depended on the size and charge of the ion with binding energies that ranged from 364 kcal mol^{-1} for the very hard Be^{2+} ion to 33 kcal mol^{-1} for the softer K^+. Further, calculations using different methodology (MP2/6-31+G*), single-point CCSD(T)/6-31+G*//MP2/6-31+G*, and single-point large basis set B3LYP/6-311++G**//B3LYP/6-31+G* calculations agree in general with B3LYP/6-31+G* results. Subtler issues to be addressed in the future may involve (i) binding selectivity between VX and Russian-VX and (ii) how stable coordination isomers can be correctly positioned for specific bond (P−S) cleavage in real catalytic systems. A long-term goal is to understand the details of how metal ion binding inhibits agent toxicity.

Acknowledgment. Funding was provided by KAIST Grant # GJ00850 (D.G.C.), the Brain Korea 21 (BK 21) program (D.G.C. and Y.S.L.) and CNMM, one of the 21st Century Frontiers Research Programs of MOST, Korea (Grant # M102KNO10010-05K1401-01J10) (Y.S.L.). Computer time was provided in part by the KISTI Supercomputer Center through the seventh Strategic Resource Support Project. Hyoseok Kim (KAIST) is gratefully acknowledged for his technical assistance.

Supporting Information Available: (i) Complete table of computed NMR values. (ii) Bond lengths and bond length distortions. (iii) Cartesian coordinates for all optimized geometries (**1**−**35**). This material is available free of charge via the Internet at http://pubs.acs.org.

References and Notes

(1) Ember, L. R. *Chem. Eng. News* **2004**, *82* (15), 28−29.
(2) Ember, L. *Chem. Eng. News* **1995**, *73* (13), 6−7.
(3) Zurer, P. *Chem. Eng. News* **1998**, *76*, 6 (35), 7.
(4) Tsuchihashi, H.; Katagi, M.; Nishikawa, M.; Tatsuno, M. *J. Anal. Toxicol.* **1998**, *22*, 383−388.
(5) Ember, L. *Chem. Eng. News* **1993**, *71* (18), 8−9.
(6) Black, R. M.; Clarke, R. J.; Read, R. W.; Reid, M. T. J. *J. Chromatogr. A* **1994**, *662*, 301−321.
(7) Ember, L. *Chem. Eng. News* **2004**, *82* (24), 15.
(8) Yang, Y. C. *Acc. Chem. Res.* **1999**, *32*, 109−115.
(9) Yang, Y. C.; Baker, J. A.; Ward, J. R. *Chem. Rev.* **1992**, *92*, 1729−1743.
(10) Mills, W. Y.; Kissling, R. M.; Gagne, M. R. *Chem. Commun.* **1999**, 1713−1714.
(11) Benschop, H. P.; De Jong, L. P. A. *Acc. Chem. Res.* **1988**, *21*, 368−374.
(12) Politzer, P.; Jayasuriya, K.; Lane, P. *Theochem* **1987**, *34*, 259−266.
(13) Patterson, E. V.; Cramer, C. J. *J. Phys. Org. Chem.* **1998**, *11*, 232−240.
(14) Rauk, A.; Shishkov, I. F.; Vilkov, L. V.; Koehler, K. F.; Kostyanovsky, R. G. *J. Am. Chem. Soc.* **1995**, *117*, 7180−7185.
(15) Albaret, C.; Lacoutiere, S.; Ashman, W. P.; Froment, D.; Fortier, P. L. *Proteins: Struct., Funct., Genet.* **1997**, *28*, 543−555.
(16) Vishnyakov, A.; Neimark, A. V. *J. Phys. Chem. A* **2004**, *108*, 1435−1439.
(17) Michalkova, A.; Ilchenko, M.; Gorb, L.; Leszczynski, J. *J. Phys. Chem. B* **2004**, *108*, 5294−5303.
(18) Šečkute, J.; Menke, J. L.; Emnet, R. J.; Patterson, E. V.; Cramer, C. J. *J. Org. Chem.* **2005**, *70*, 8649.
(19) Wagner, G. W.; Bartram, P. W. *Langmuir* **1999**, *15*, 8113−8118.
(20) Wagner, G. W.; Procell, L. R.; O'Connor, R. J.; Munavalli, S.; Carnes, C. L.; Kapoor, P. N.; Klabunde, K. J. *J. Am. Chem. Soc.* **2001**, *123*, 1636−1644.
(21) Wagner, G. W.; Bartram, P. W.; Koper, O.; Klabunde, K. J. *J. Phys. Chem. B* **1999**, *103*, 3225−3228.
(22) Wagner, G. W.; Procell, L. R.; Yang, Y. C.; Bunton, C. A. *Langmuir* **2001**, *17*, 4809−4811.
(23) Guilbault, G. G.; Affolter, J.; Tomita, Y.; Kolesar, E. S., Jr. *Anal. Chem.* **1981**, *53*, 2057−2060.
(24) Mackay, R. A.; Poziomek, E. J. *Inorg. Chem.* **1981**, *20*, 3111−3112.
(25) Van Den Berg, G. R.; Beck, H. C.; Benschop, H. P. *Bull. Environ. Contam. Toxicol.* **1984**, *33*, 505−514.
(26) Xie, Y. W.; Popov, B. N. *Anal. Chem.* **2000**, *72*, 2075−2079.
(27) Nieuwenhuizen, M. S.; Harteveld, J. L. N. *Talanta* **1994**, *41*, 461−472.
(28) Nieuwenhuizen, M. S.; Harteveld, J. L. N. *Sens. Actuator B−Chem.* **1997**, *40*, 167−173.
(29) Becke, A. D. *J. Chem. Phys.* **1993**, *98*, 5648−5652.
(30) Lee, C. T.; Yang, W. T.; Parr, R. G. *Phys. Rev. B* **1988**, *37*, 785−789.
(31) Boys, S. F.; Bernardi, F. *Mol. Phys.* **1970**, *19*, 553−566.
(32) Frisch, M. J.; Trucks, G. W.; Schlegel, H. B.; Scuseria, G. E.; Robb, M. A.; Cheeseman, J. R.; Montgomery, Jr., J. A.; Vreven, T.; Kudin, K. N.; Burant, J. C.; Millam, J. M.; Iyengar, S. S.; Tomasi, J.; Barone, V.; Mennucci, B.; Cossi, M.; Scalmani, G.; Rega, N.; Petersson, G. A.; Nakatsuji, H.; Hada, M.; Ehara, M.; Toyota, K.; Fukuda, R.; Hasegawa, J.; Ishida, M.; Nakajima, T.; Honda, Y.; Kitao, O.; Nakai, H.; Klene, M.; Li, X.; Knox, J. E.; Hratchian, H. P.; Cross, J. B.; Adamo, C.; Jaramillo, J.; Gomperts, R.; Stratmann, R. E.; Yazyev, O.; Austin, A. J.; Cammi, R.; Pomelli, C.; Ochterski, J. W.; Ayala, P. Y.; Morokuma, K.; Voth, G. A.; Salvador, P.; Dannenberg, J. J.; Zakrzewski, V. G.; Dapprich, S.; Daniels, A. D.; Strain, M. C.; Fartas, O.; Malick, D. K.; Rabuck, A. D.; Raghavachari, K.; Foresman, J. B.; Ortiz, J. V.; Cui, Q.; Baboul, A. G.; Clifford, S.; Cioslowski, J.; Stefanov, B. B.; Liu, G.; Liashenko, A.; Piskorz, P.; Komaromi, I.; Martin, R. L.; Fox, D. J.; Keith, T.; Al-Laham, M. A.; Peng, C. Y.; Nanayakkara, A.; Challacombe, M.; Gill, P. M. W.; Johnson, B.; Chen, W.; Wong, M. W.; Gonzalez, C.; Pople, J. A. *Gaussian 03*, revision A.1 ed.; Gaussian, Inc.: Pittsburgh, PA, 2003.
(33) Mehlsen Soerensen, A. *Acta Crystallogr., B* **1977**, *B33*, 2693−2695.
(34) Hancock, R. D.; Martell, A. E. *Chem. Rev.* **1989**, *89*, 1875−1914.
(35) Bondi, A. *J. Phys. Chem.* **1964**, *68*, 441−452.
(36) Mikuriya, M.; Okawa, H.; Kida, S. *Bull. Chem. Soc. Jpn.* **1980**, *53*, 2871−2877.
(37) Mikuriya, M.; Okawa, H.; Kida, S. *Bull. Chem. Soc. Jpn.* **1981**, *54*, 2979−2982.
(38) Mikuriya, M.; Okawa, H.; Kida, S. *Bull. Chem. Soc. Jpn.* **1982**, *55*, 1086−1091.
(39) Jain, V. K.; Chaudhury, S.; Bohra, R. *Polyhedron* **1993**, *12*, 2377−2385.
(40) Mikuriya, M.; Toriumi, K.; Ito, T.; Kida, S. *Inorg. Chem.* **1985**, *24*, 629−631.
(41) Casals, I.; Gonzalez-Duarte, P.; Lopez, C.; Solans, X. *Polyhedron* **1990**, *9*, 763−768.
(42) (a) Please refer to the Supporting Information for a complete list of P═O, C−S, P−OR, and P−S bond lengths and their changes with respect to the bond lengths in VX−Me. (b) Please refer to the Supporting Information for a complete table of calculated NMR values.
(43) Yang, Y. C.; Szafraniec, L. L.; Beaudry, W. T.; Rohrbaugh, D. K.; Procell, L. R.; Samuel, J. B. *J. Org. Chem.* **1996**, *61*, 8407−8413.
(44) Yang, Y. C.; Szafraniec, L. L.; Beaudry, W. T.; Rohrbaugh, D. K. *J. Am. Chem. Soc.* **1990**, *112*, 6621−6627.
(45) Panda, M.; Phuan, P.-W.; Kozlowski, M. C. *Chem. Commun.* **2002**, 1552−1553.
(46) Bannister, E.; Cotton, F. A. *J. Chem. Soc. 2* **1960**, 2276−2280.
(47) Cotton, F. A.; Goodgame, D. M. L. *J. Am. Chem. Soc.* **1960**, *82*, 5771−5773.
(48) (a) The Cambridge Structural Database, version 5.26. (b) Allen, F. H. *Acta Cryst.* **2002**, *B58*, 380−388.3